Supplemental Table 1

Antibodies used for the detection of leukocyte subsets in the human brain

Antigen	Cellular expression	Function
CD8	Thymocyte subsets, cytotoxic T-cells	co-receptor for MHC class I
CD4	Thymocyte subsets, helper and inflammatory T-cells	co-receptor for MHC class II
CD79α	B-cells	component of the B-cell receptor complex
CD20	B-cells	putative calcium channel
CD57	natural killer cell	human lymphocyte oligosaccharide antigen

Supplemental Table 2

T-cell density in the red nucleus (cells/mm^2)

	Controls	PD
$CD8^+$	0.245 ± 0.040	0.155 ± 0.090
$CD4^+$	0.021 ± 0.014	0.009 ± 0.005

$CD8^+$ and $CD4^+$ T-cell density in controls and PD patients do not differ (*P* = 0.34 and *P* = 0.71, respectively; Student's *t* test). Data represent means ± SEM

Supplemental Figure 1

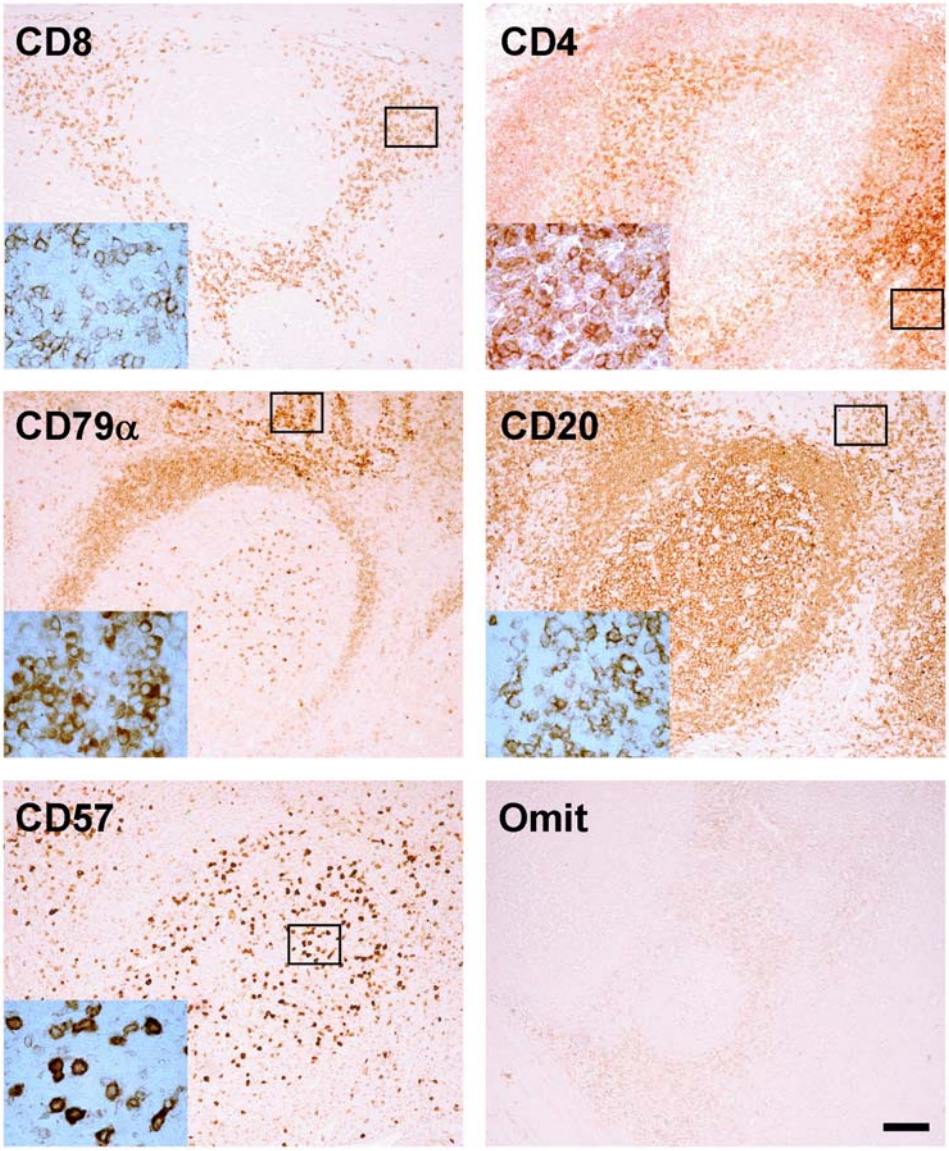

Supplemental Figure 1: Immunohistochemical detection of leukocyte subsets in human tonsil control tissue. Representative photomicrographs of human tonsil tissue sections immunostained for either CD8, CD4, CD79a, CD20 or CD57. Inset: higher magnification view of the boxed areas. A positive cellular staining was obtained for each of these leukocyte markers attesting the validity of the methodology used for the detection of lymphocyte subsets in our *postmortem* human brain material. Note that omission of the primary antibody resulted in absence of staining (Omit). Scale bar: 100 µm (insets: 30 µm).

Supplemental Figure 2

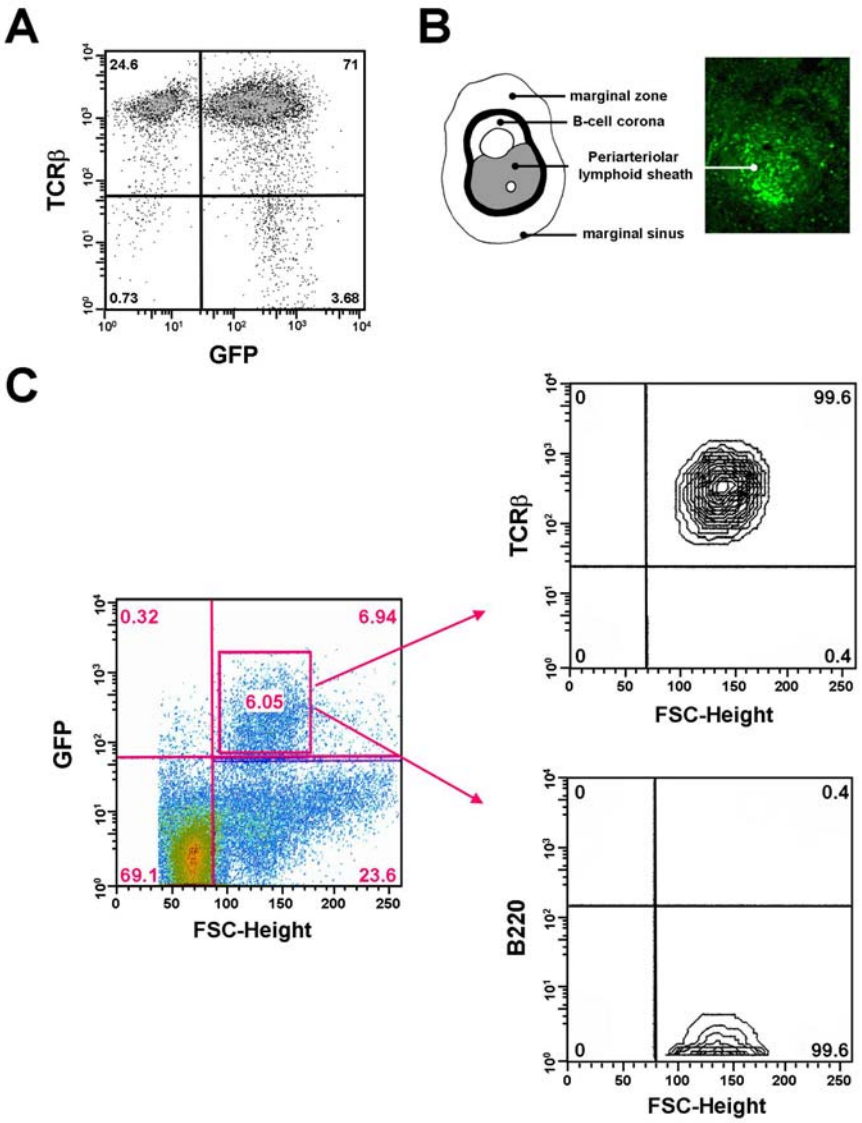

Supplemental Figure 2: Characterization of GFP+ T-cell-reconstituted *Rag1*-/- mice (**a**) Flow cytometry analysis of TCRb and GFP expression in positively selected cells from Tie2-Cre+/ZEG+ mouse lymph nodes shows more than 95% enrichment in T-cells. (**b**) Schematic view of white pulp in a transverse section of mouse spleen (left). Note that the periarteriolar lymphoid sheath (PALS) is made up of T cells. (Right) GFP+ cells in a transverse section of spleen from a GFP+ T-cell-reconstituted *Rag1*-/- mouse at 4 weeks post-transfer. Most of the GFP+ cells are located within the PALS. (**c**) Representative frequency of T- (TCRb+) and B-cells (B220+) among gated GFP+ cell subsets in lymph nodes from a MPTP-treated GFP+ T-cell-reconstituted *Rag1*-/- mouse. GFP+ cells are almost exclusively of T-cell subtype without major B-cell contamination.

Supplemental Figure 3

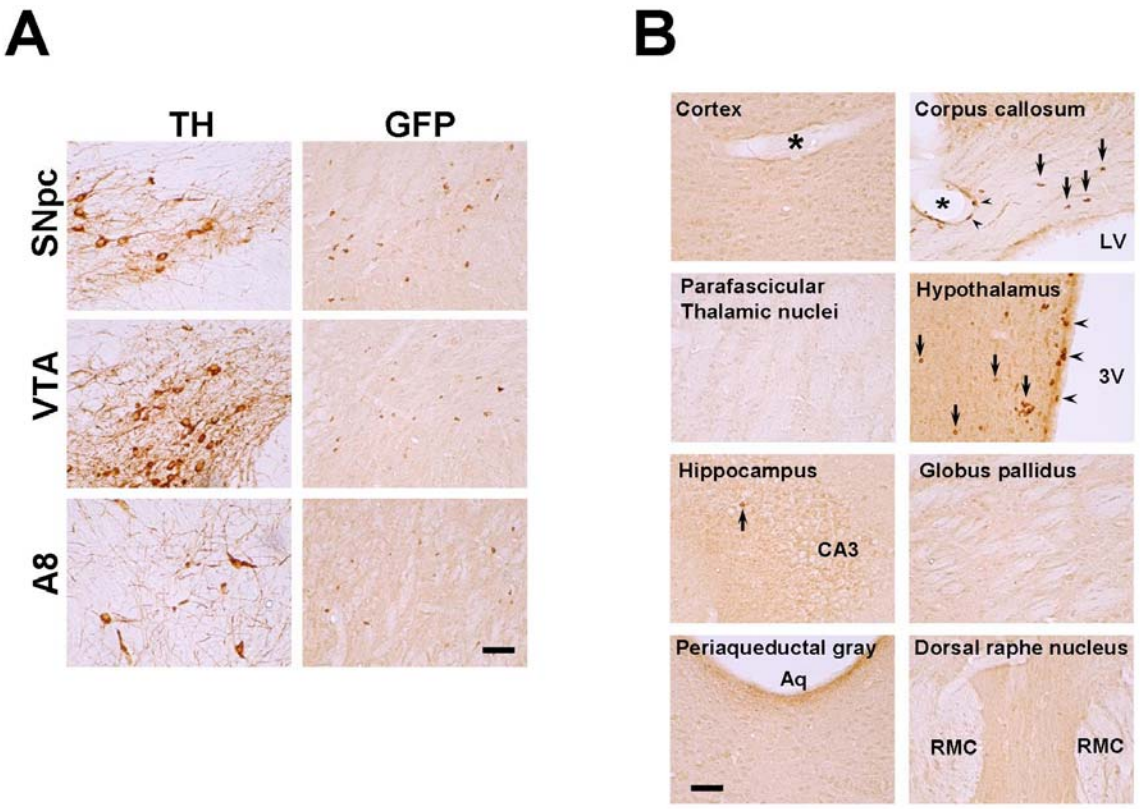

Supplemental Figure 3: Site specific recruitment of GFP+ T-cells in the brain of MPTP-intoxicated mice. (**a**) GFP+ T-cell infiltration (sections immunostained for GFP, right panels) in DN-containing brain areas (sections immunostained for TH, left panels) including the SNpc, the catecholaminergic cell group A8 and the ventral tegmental area (VTA). Scale bar: 80 µm. (**b**) MPTP-induced T-cell extravasation in various brain areas. Except in the corpus callosum and hypothalamus, infiltrated GFP+ T-cells (arrows) are rarely found in other brain structures. Asterisk: blood vessels, LV, lateral ventricle, 3V, third ventricle, Aq, Sylvius aqueduct, RMC, magnocellular part of the red nucleus. Scale bar: 80 µm.

Supplemental Figure 4

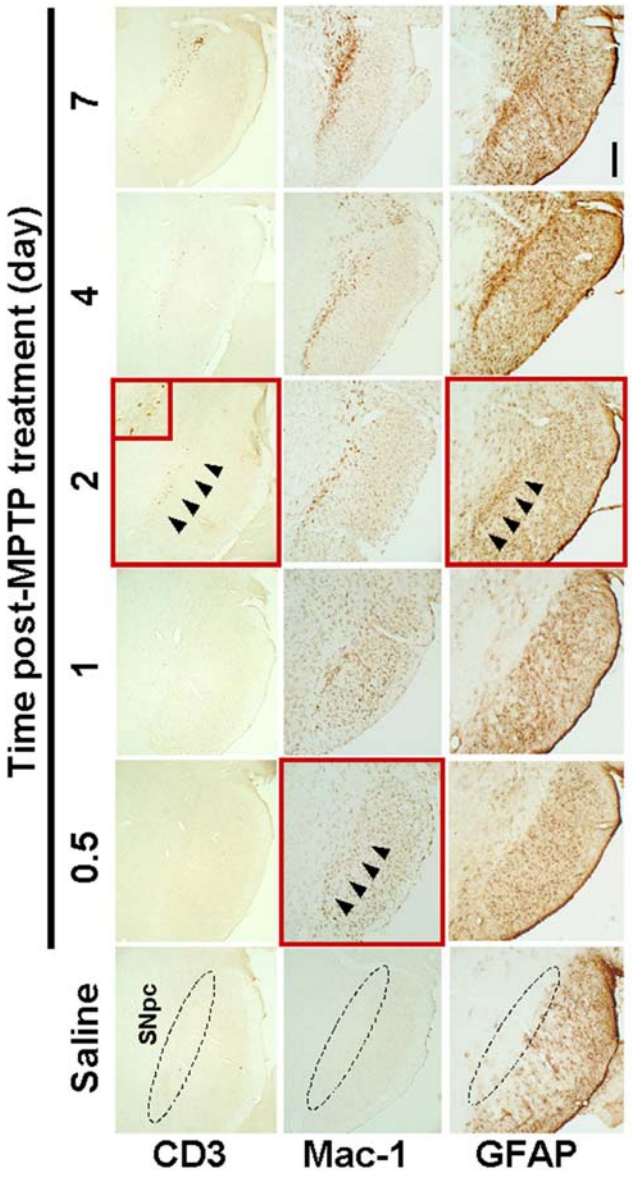

Supplemental Figure 4: Kinetics of T-cell brain infiltration and glial cell activation in the SNpc of MPTP-intoxicated mice. Representative photomicrographs of mesencephalic sections immunostained for CD3 (upper panels), Mac-1/CD11b (middle panels) and GFAP (lower panels) from saline- or MPTP-treated mice sacrificed at 12hr, 1, 2, 4 and 7 days after toxin exposure. The SNpc is delineated by dashed line. Red-circled photomicrographs indicate the earliest time point at which CD3+ T-cells, Mac-1+ activated microglial cells or GFAP+ astrocytes can be substantially detected in the SNpc (arrowheads). Inset in day 2 CD3 picture shows CD3+ T-cells at higher magnification. Note that microglial cell activation following MPTP-induced nigrostriatal pathway injury precedes T-cell infiltration and astrogliosis. Scale bar: 300 µm.

Supplemental Figure 5

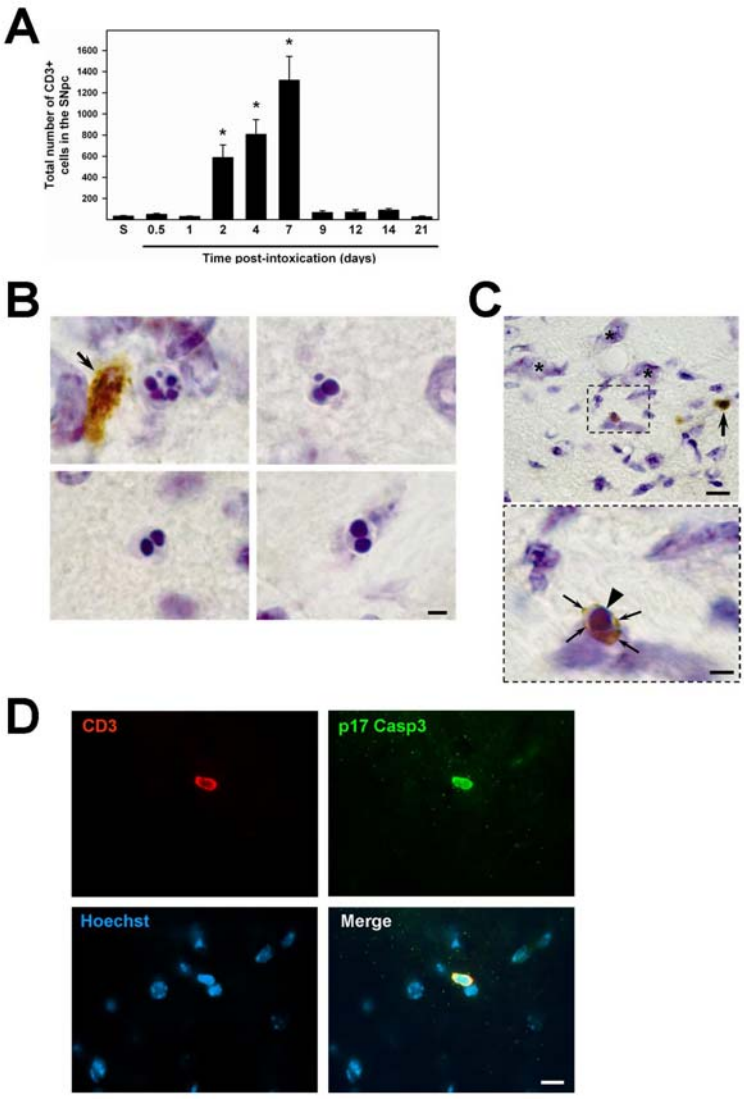

Supplemental Figure 5: Evidences for CD3+ T-cell apoptosis in the SNpc following MPTP intoxication. (**a**) Quantification of the total number of CD3+ T-cells in the SNpc at different time points after MPTP exposure. S: saline-treated controls. Each data point represents the mean ± SEM of 5-13 brains per group. *, $P < 0.01$, compared with saline-treated controls (Tukey *post hoc* analysis). (**b**) CD3 immunostaining with thionin counterstaining on mesencephalic sections from MPTP-treated mice sacrificed at day 7 and day 9 after intoxication. Photomicrographs at the level of the SNpc showing cases of pyknotic cells with well-defined thionin-stained chromatin clumps. A CD3+ T cell (arrow) with well preserved thionin-stained nucleus is shown in the vicinity of an apoptotic cell. Scale bar: 4 µm (**c**) Same experimental conditions as in (b). Illustration of a CD3+ apoptotic cell within the SNpc at day 7 after MPTP. Arrow: normal CD3+ T cell, Asterisks: neurons. Magnification of the dashed box area shows a T cell with CD3 staining (arrows) and a condensed thionin-stained nucleus typical of apoptosis. Scale bar: 10 µm, dashed box: 4 µm. (**d**). Double immunofluorescent staining for CD3 (red) and p17 caspase-3 (green) with Hoechst counterstaining (blue). Scale bar: 8 µm.

Supplemental Figure 6

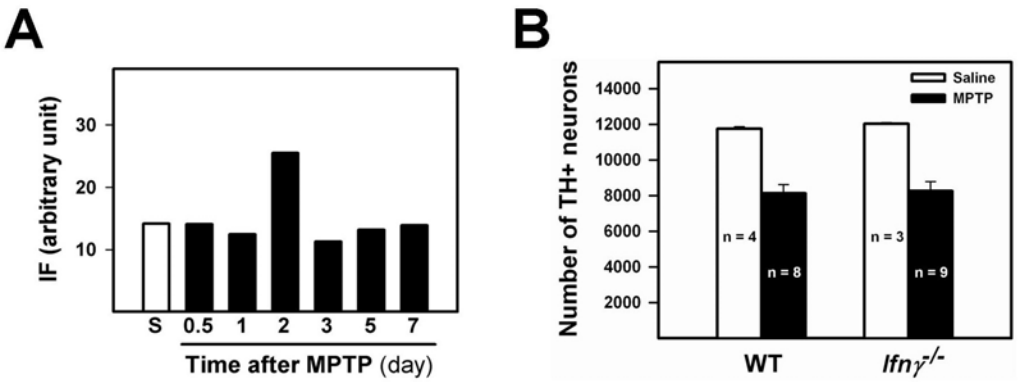

Supplemental Figure 6: Expression and role of IFN-γ in MPTP-induced nigrostriatal pathway injury. (**a**) Time course of IFN-γ expression in the ventral midbrain following MPTP intoxication as determined using antibody array glass chip (see Methods for details). IF: intensity of fluorescence, S: saline-treated mice. Note the up-regulated expression of IFN-γ two days after MPTP exposure. (**b**) Quantification of total TH+ DN neurons in the SNpc at day 7 after MPTP (4x18mg/kg) or saline treatment in WT and *Ifnγ*-/- mice. Data represent the mean number of total nigral TH+ DNs ± SEM for the indicated number of animals. Mice deficient in IFN-γ and their WT littermates are equally sensitive to MPTP-induced dopaminergic cell death ($P = 0.85$, Student's *t* test).